Force Maximization of Biarticularly Actuated Manipulators Using Infinity Norm

Valerio Salvucci, *Member, IEEE*, Yasuto Kimura, Sehoon Oh, *Member, IEEE*, and Yoichi Hori, *Fellow, IEEE*

Abstract—There is a rising interest in biologically inspired manipulators equipped with biarticular actuators—actuators that span two joints—for solving the known limitations of conventional systems. In contrast with kinematic redundancy, actuator redundancy resulting from the presence of biarticular actuators has the added advantages of bringing more stability, reducing the inertia of the robot links, and decreasing the nonlinearity of the end effector force as a function of force direction. In this paper, the advantage of the infinity norm optimization criteria on a robot designed under the actuator redundancy paradigm is investigated. A closed form solution based on the infinity norm for a manipulator with mono- and biarticular actuators is derived. The proposed infinity norm-based approach is compared with the conventional method based on pseudoinverse matrix by both calculation and experiment. Under the same actuator limitations, the maximum end effector force produced with the proposed method is significantly greater than the one produced by the conventional method. The proposed closed form solution is suitable for redundant systems with three inputs and two outputs, bringing the advantage of an higher maximum output without the need for iterative algorithms.

Index Terms—Control systems, manipulators, robots.

I. INTRODUCTION

ROBOT manipulators presenting animal musculoskeletal characteristics such as biarticular actuators—actuators that span two joints—have been proposed for more than two decades [1].

From a control point of view, biarticularly actuated robots often present more actuators than joints, resulting in actuator redundancy. The resolution of actuator redundancy represents a key point in the control design for such robots.

Approaches based on pseudoinverse matrices are used in the control design for kinematically redundant manipulator [2]–[4]. Pseudoinverse matrices are also used for actuator redundancy resolution [5]–[7]. Moore–Penrose is the simplest pseudoinverse matrix, and correspond to the minimization of the euclidean norm [8].

Iterative algorithms based on ∞-norm optimization criteria have been used to resolve redundancy in kinematically redundant manipulators [9]–[12]. In this paper, the ∞-norm is used to resolve the actuator redundancy for biarticularly actuated robot arms. A closed form solution based on a piecewise linear function for the infinity-norm approach is proposed. This piecewise linear function is valid also for the case in which the maximum joint actuator torques are not the same, but differ form each other.

The ∞-norm approach is compared with the Moore–Penrose pseudoinverse approach (2-norm in the following) in terms of maximum output force at the end effector by using both calculation and experimental methods. The ∞-norm approach maximizes the force at the end effector given the joint actuator torque limitations. As a consequence, under the same joint actuator torque limitations, the maximum output force at the end effector calculated using the ∞-norm approach is greater than the one obtained using the 2-norm approach. Conversely, given a desired output force at the end effector, the maximum joint actuator torque required by using the ∞-norm approach is smaller. Therefore, the proposed approach is suitable to optimize the design of biarticularly actuation in manipulators.

The experimental validation of the proposed approach is realized using BiWi, a biarticularly actuated and Wire driven robot arm.

Modeling and advantages of biarticularly actuated manipulators are described in Section II. In Sections III and IV, the redundancy actuator problem and the resolution approaches based on 2-norm and ∞-norm are illustrated. In Section V, the BiWi robot arm is described together with the feedforward control strategy used in the experiment. In Section VI, the proposed ∞-norm approach is compared with 2-norm approach in terms of maximum output force at the end effector by both calculation and experimental methods. Finally, in Section VII, the advantages of the ∞-norm approach are summarized. The proof of the closed form solution of the 2-norm and ∞-norm approaches are reported in Appendix and Appendix, respectively.

II. MODELING OF BIARTICULARLY ACTUATED MANIPULATORS

In conventional manipulators each joint is driven by one actuator. On the other hand, animal and human limbs present a complex musculoskeletal structure based on mono- and multiarticular muscles.

1) Monoarticular muscles produce a torque on one joint.
2) Multiarticular muscles span more than one joint. Gastrocnemius is an example of biarticular muscle in the human leg.
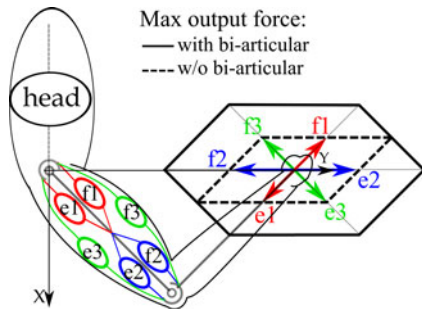
Fig. 1. Two-link arm with four mono- and two biarticular actuators: model and resulting forces at the end effector.

TABLE I
MUSCLES' NAMES, TYPES AND SYMBOLS

Name	Type	Symbol
Deltoid, posterior part	mono	e1
Deltoid, anterior part	mono	f1
Triceps, lateral head	mono	e2
Brachialis	mono	f2
Triceps, long head	bi	e3
Biceps brachii	bi	f3

A widely used simplified model of the complex animal musculoskeletal system [13]– [17] is shown in Fig. 1. The muscles' name, type, and relative symbol are illustrated in Table I. This model is based on six contractile actuators—three extensors (e1, e2, and e3) and three flexors (f1, f2, and f3)—coupled in three antagonistic pairs:

1) e1–f1 and e2–f2: couples of monoarticular actuators that produce torques about joint 1 and 2, respectively;
2) e3–f3: couple of biarticular actuators that produce torque about joint 1 and 2 contemporaneously.

Every of the six muscles produce a force e_i or f_i with respective maximum force $e_i^{\max}$ or $f_i^{\max}$ for $i = (1, 2, 3)$.

The resulting forces at the end effector are shown in Fig. 1. If only monoarticular muscles are considered, there are four resulting forces at the end effector and the maximum output force space is a quadrilateral. On the other hand, if biarticular actuators are added, there are six forces at the end effector, hence the maximum output force space becomes an hexagon.

A. Advantages of Biarticular Actuation

Biarticular actuators bring numerous advantages in robot applications. First, biarticular actuators dramatically increase the range of end effector impedance that can be achieved without feedback [1]. Consequences are, for example, capability of path tracking and disturbance rejection using just feedforward control [18], [19], and the improvement of balance control for legged robots without force sensors [20].

Biarticular actuators transfer mechanical energy from proximal to distal joints [21]. This is a key aspect in legged robots for hopping [22]–[24], for jumping [25], and for running [26], as well for power-assist robots [27], [28].

Biarticularly actuated manipulators produce a maximum output force at the end effector in a more homogeneous distributed way [29]. The maximum output force at the end effector for
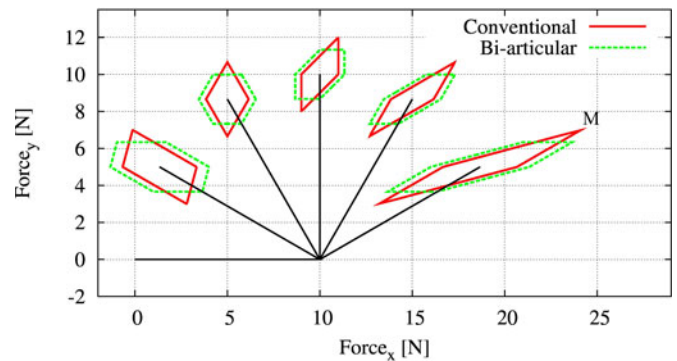

Fig. 2. Maximum output force at the end effector for conventional and biarticularly driven arm.
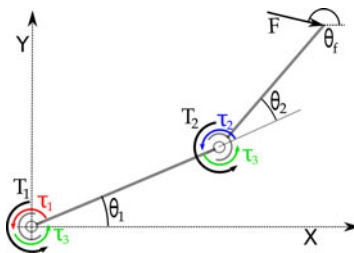

Fig. 3. Statics of two-link arm with four mono- and two biarticular actuators.

a two-link conventional manipulator and for a biarticularly actuated robot arm is shown in Fig. 2 for comparison. The conventional manipulator has two actuators with maximum joint actuator torques $T_1 = T_2 = 10$ Nm, and the biarticularly actuated robot arm has three actuators with maximum joint actuator torques $\tau_1 = \tau_2 = \tau_3 = 6.66$ Nm. All the gear ratios of all the actuators are the same. Therefore, the sum of maximum actuator torques are the same (i.e., 20 Nm) in the two cases. The conventional quadrilateral shape becomes an hexagon for biarticularly driven arms, which, therefore, produces a maximum force at the end effector more homogeneously distributed in respect to output force direction. The maximum output force that can be physically produced by applications that interact with humans is a key aspect in safety. There are power assist robots in which pneumatic actuators [30], [31], elastic elements [32], [33], or linear motor [34] are used to increase backdrivability and, therefore, safety for the users. Peak output forces such as the one in point M in Fig. 2 cannot be produced by the human arm, therefore are unnecessary and dangerous in case of failure of the controller. As a consequence, the use of biarticular actuators further increases safety for power assist robots [35], [36].

In addition to these advantages, multiarticular actuators, such as triarticular actuators, increase the efficiency in output force generation, as for example in lancelet-like swimming robots [17].

III. ACTUATOR REDUNDANCY PROBLEM

The resulting statics of the biarticularly actuated arm of Fig. 1 are shown in Fig. 3, where:

1) The total torques about joint 1 and 2 are T_1 and T_2, respectively.

2) The torques produced by monoarticular actuators about joints 1 and 2 are τ_1 and τ_2, respectively. They are calculated from the actuator input forces e_i and f_i for $i = (1, 2)$ as follows:

$$\tau_1 = (f_1 - e_1)r \tag{1}$$

$$\tau_2 = (f_2 - e_2)r \tag{2}$$

where r is the distance between the joint axis and the point where the muscle force is applied. The value of r is consider to be the same for all the muscles and all joint angles.

3) The torque produced about both joints by biarticular actuators is τ_3

$$\tau_3 = (f_3 - e_3)r. \tag{3}$$

4) $\boldsymbol{F}$ is a general force at the end effector with magnitude F and direction θ_f.

The statics of this system are therefore expressed by

$$T_1 = \tau_1 + \tau_3 \tag{4}$$

$$T_2 = \tau_2 + \tau_3. \tag{5}$$

A two-link manipulator with the statics shown in Fig. 3 presents actuator redundancy. Given τ_1, τ_2, and τ_3, it is possible to determine $\boldsymbol{T}$, and therefore $\boldsymbol{F}$ by using the Jacobian

$$\begin{bmatrix} T_1 \\ T_2 \end{bmatrix} = J^T \begin{bmatrix} F_x \\ F_y \end{bmatrix} \tag{6}$$

where

$$J = \begin{bmatrix} -l_1\sin(\theta_1) - l_2\sin(\theta_1 + \theta_2) & -l_2\sin(\theta_1 + \theta_2) \\ l_1\cos(\theta_1) + l_2\cos(\theta_1 + \theta_2) & l_2\cos(\theta_1 + \theta_2) \end{bmatrix} \tag{7}$$

and F_x and F_y are the orthogonal projection of $\boldsymbol{F}$ on the x-axis and y-axis, respectively. On the other hand, given $\boldsymbol{F}$, and therefore $\boldsymbol{T}$, it is generally not possible to determine uniquely τ_1, τ_2, and τ_3 [see (4) and (5)] due to the actuator redundancy. The problem represented by (4) and (5) is referred in the following as the redundancy actuator problem.

The 2-norm and the ∞-norm approaches are described in the following.

IV. APPROACHES FOR ACTUATOR REDUNDANCY RESOLUTION

Given the arm with the statics as in Fig. 3 and a desired force at the end effector $\boldsymbol{F}$, the desired joint torques $\boldsymbol{T}$ are calculated using (6), and the three desired joint actuator torques τ_1, τ_2, and τ_3 that produces $\boldsymbol{T}$ are calculated using the 2-norm and the ∞-norm approaches as described in Section IV-A and Section IV-B, respectively.

A. 2-Norm-Based Approach

The actuator redundancy is resolved using the 2-norm by solving the following problem:

$$\min \quad \sqrt{\frac{(\tau_1)^2}{(\tau_1^{\max})^2} + \frac{(\tau_2)^2}{(\tau_2^{\max})^2} + \frac{(\tau_3)^2}{(\tau_3^{\max})^2}}$$

$$\text{s.t.} \quad T_1 = \tau_1 + \tau_3$$

$$T_2 = \tau_2 + \tau_3 \tag{8}$$

where $\tau_i^{\max}, i = (1, 2, 3)$ is the maximum joint actuator torque that the actuator i can produce.

The solution of the problem expressed by (8) is

$$\tau_1 = \frac{(T_1 - T_2)(\tau_1^{\max})2(\tau_3^{\max})^2 + T_1(\tau_1^{\max})^2(\tau_2^{\max})^2}{(\tau_1^{\max})^2(\tau_2^{\max})^2 + (\tau_1^{\max})^2(\tau_3^{\max})^2 + (\tau_2^{\max})^2(\tau_3^{\max})^2} \tag{9}$$

$$\tau_2 = \frac{T_2(\tau_1^{\max})^2(\tau_2^{\max})^2 + (T_2 - T_1)(\tau_2^{\max})^2(\tau_3^{\max})^2}{(\tau_1^{\max})^2(\tau_2^{\max})^2 + (\tau_1^{\max})^2(\tau_3^{\max})^2 + (\tau_2^{\max})^2(\tau_3^{\max})^2} \tag{10}$$

$$\tau_3 = \frac{T_1(\tau_2^{\max})^2(\tau_3^{\max})^2 + T_2(\tau_1^{\max})^2(\tau_3^{\max})^2}{(\tau_1^{\max})^2(\tau_2^{\max})^2 + (\tau_1^{\max})^2(\tau_3^{\max})^2 + (\tau_2^{\max})^2(\tau_3^{\max})^2}. \tag{11}$$

Proof of (9), (10), and (11) is reported in Appendix A.

If $\tau_1^{\max} = \tau_2^{\max} = \tau_3^{\max}$ the solution becomes

$$\tau_1 = \frac{2}{3}T_1 - \frac{1}{3}T_2 \tag{12}$$

$$\tau_2 = -\frac{1}{3}T_1 + \frac{2}{3}T_2 \tag{13}$$

$$\tau_3 = \frac{1}{3}T_1 + \frac{1}{3}T_2. \tag{14}$$

B. Infinity Norm-Based Approach

The actuator redundancy is resolved using the ∞-norm by solving the following problem:

$$\min \quad \max \left(\frac{|\tau_1|}{\tau_1^{\max}}, \frac{|\tau_2|}{\tau_2^{\max}}, \frac{|\tau_3|}{\tau_3^{\max}} \right)$$

$$\text{s.t.} \quad T_1 = \tau_1 + \tau_3$$

$$T_2 = \tau_2 + \tau_3. \tag{15}$$

The fact that three torque values are scaled by the respective maximum torque guarantees that the solution, when exists, does not violate any of the three constraints:

$$-\tau_1^{\max} \le \tau_1 \le \tau_1^{\max} \tag{16}$$

$$-\tau_2^{\max} \le \tau_2 \le \tau_2^{\max} \tag{17}$$

$$-\tau_3^{\max} \le \tau_3 \le \tau_3^{\max}. \tag{18}$$

Let us define

$$c_1 = \frac{\tau_3^{\max} - \tau_1^{\max}}{\tau_3^{\max} + \tau_2^{\max}} \tag{19}$$

$$c_2 = \frac{\tau_3^{\max} + \tau_2^{\max}}{\tau_3^{\max} + \tau_1^{\max}} \tag{20}$$

$$c_3 = \frac{\tau_3^{\max} - \tau_2^{\max}}{\tau_3^{\max} + \tau_1^{\max}}. \tag{21}$$

The three parameters c_1, c_2, and c_3 defined for any maximum joint actuator torque, and are constant. A closed form solution of the problem (15) is determined on the basis of the values of T_1 and T_2 as follows:

$$\tau_1 = \begin{cases} (T_1 - T_2)\dfrac{\tau_1^{\max}}{\tau_1^{\max} + \tau_2^{\max}} & \text{if case}_1 \\[2mm] T_1 - T_2\dfrac{\tau_3^{\max}}{\tau_2^{\max} + \tau_3^{\max}} & \text{if case}_2 \\[2mm] T_1\dfrac{\tau_1^{\max}}{\tau_1^{\max} + \tau_3^{\max}} & \text{if case}_3 \end{cases} \tag{22}$$

$$\tau_2 = \begin{cases} (T_2 - T_1)\dfrac{\tau_2^{\max}}{\tau_1^{\max} + \tau_2^{\max}} & \text{if case}_1 \\[2mm] T_2\dfrac{\tau_2^{\max}}{\tau_2^{\max} + \tau_3^{\max}} & \text{if case}_2 \\[2mm] T_2 - T_1\dfrac{\tau_3^{\max}}{\tau_1^{\max} + \tau_3^{\max}} & \text{if case}_3 \end{cases} \tag{23}$$

$$\tau_3 = \begin{cases} \dfrac{T_1\tau_2^{\max} + T_2\tau_1^{\max}}{\tau_1^{\max} + \tau_2^{\max}} & \text{if case}_1 \\[2mm] T_2\dfrac{\tau_3^{\max}}{\tau_2^{\max} + \tau_3^{\max}} & \text{if case}_2 \\[2mm] T_1\dfrac{\tau_3^{\max}}{\tau_1^{\max} + \tau_3^{\max}} & \text{if case}_3 \end{cases} \tag{24}$$

where

$$\begin{aligned} \text{case}_1 &= (T_1 \le c_1 T_2 \text{ and } T_2 \ge c_3 T_1) \\ &\quad \text{or } (T_1 > c_1 T_2 \text{ and } T_2 < c_3 T_1) \\ \text{case}_2 &= (T_1 \ge c_1 T_2 \text{ and } T_2 \ge c_2 T_1) \\ &\quad \text{or } (T_1 < c_1 T_2 \text{ and } T_2 < c_2 T_1) \\ \text{case}_3 &= (T_2 \le c_2 T_1 \text{ and } T_2 \ge c_3 T_1) \\ &\quad \text{or } (T_2 > c_2 T_1 \text{ and } T_2 < c_3 T_1). \end{aligned}$$

Proofs of (22), (23), and (24) are reported in Appendix B.

It is trivial to verify that the three linear piecewise functions (22), (23), and (24) are continuous in all the domain $D = (T_1, T_2)$.

In summary, the values of τ_1, τ_2, and τ_3 that produce a given $\boldsymbol{F}$ at the end effector, are determined as follows.
1) Calculate the desired joint torques $\boldsymbol{T} = J^T \boldsymbol{F}$.
2) According to calculated T_1 and T_2, the three desired joint actuator torques are directly determined using the three piecewise linear function (22), (23), and (24).

When all the actuators produce the same maximum joint actuator torque, that is $\tau_1^{\max} = \tau_2^{\max} = \tau_3^{\max}$, $c_1 = c_3 = 0$ and
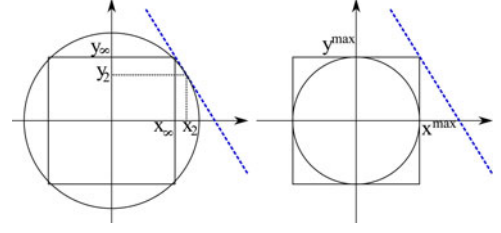

Fig. 4. Graphical comparison between ∞-norm and 2-norm: solution comparison (left), no solution for 2-norm (right).

$c_2 = 1$, and the solution becomes as in the following [37], [38]:

$$\tau_1 = \begin{cases} \dfrac{T_1 - T_2}{2} & \text{if } T_1 T_2 \le 0 \\[2mm] T_1 - \dfrac{T_2}{2} & \text{if } T_1 T_2 > 0 \quad \text{and} \quad |T_1| \le |T_2| \\[2mm] \dfrac{T_1}{2} & \text{if } T_1 T_2 > 0 \quad \text{and} \quad |T_1| > |T_2| \end{cases} \tag{25}$$

$$\tau_2 = \begin{cases} \dfrac{T_2 - T_1}{2} & \text{if } T_1 T_2 \le 0 \\[2mm] \dfrac{T_2}{2} & \text{if } T_1 T_2 > 0 \quad \text{and} \quad |T_1| \le |T_2| \\[2mm] T_2 - \dfrac{T_1}{2} & \text{if } T_1 T_2 > 0 \quad \text{and} \quad |T_1| > |T_2| \end{cases} \tag{26}$$

$$\tau_3 = \begin{cases} \dfrac{T_1 + T_2}{2} & \text{if } T_1 T_2 \le 0 \\[2mm] \dfrac{T_2}{2} & \text{if } T_1 T_2 > 0 \text{ and } |T_1| \le |T_2| \\[2mm] \dfrac{T_1}{2} & \text{if } T_1 T_2 > 0 \text{ and } |T_1| > |T_2|. \end{cases} \tag{27}$$

C. Infinity-Norm Approach: The Reason Why

Fig. 4 shows the graphical comparison between ∞-norm and 2-norm optimization criteria in selecting the optimal solution for a problem in $\mathbb{R}^2$. The dashed line represents the infinite set of solutions (x, y) that satisfy

$$k = \alpha x + y \tag{28}$$

where α represent the relationship between the desired output k and the necessary inputs x and y. The positive constants $x^{\max}$ and $y^{\max}$ define the allowable ranges for x and y:

$$-x^{\max} \le x \le x^{\max} \tag{29}$$

$$-y^{\max} \le y \le y^{\max}. \tag{30}$$

The two sets (x_2, y_2) and (x_∞, y_∞) in Fig. 4 (left) are the two solutions of (28) calculated using the 2-norm (the circle) and ∞-norm (the square) optimization criteria, respectively. By definition, the infinity norm minimize the maximum input, therefore, it holds that

$$\max\{|x_\infty|, |y_\infty|\} \le \max\{|x_2|, |y_2|\}. \tag{31}$$

Therefore, if x and y are bounded as in (29) and (30), the ∞-norm model admits solution for higher values of k than the 2-norm, as shown in Fig. 4 (right).
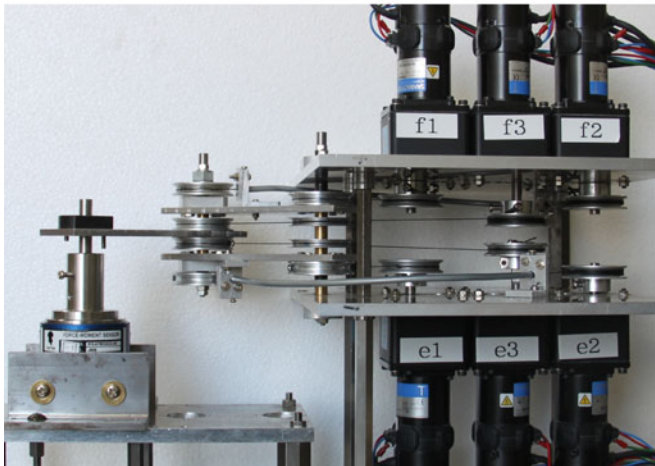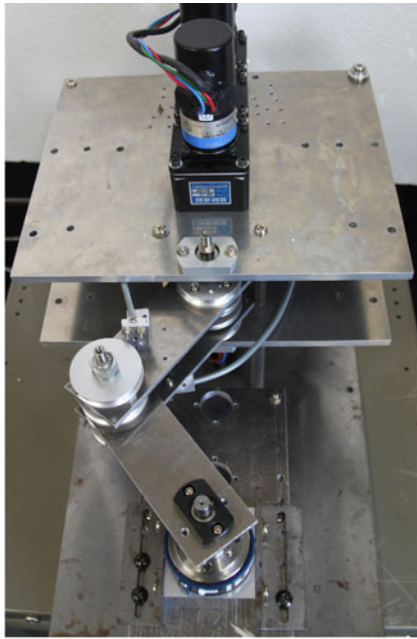
Fig. 5. BiWi, a biarticulated driven and wire driven robotic arm: top view (top), side view (bottom) [39].

Fig. 6. Torque transmission system.

TABLE II
BiWi CHARACTERISTICS

Parameter	Value
Link 1	112 [mm]
Link 2	112 [mm]
Pulleys diameter (all)	44 [mm]
Thrust wire	30 [mm]

TABLE III
ACTUATOR AND SENSOR SYSTEM

Motors	Sanyo T404-012E59
Gear head	G6-12 (ratio 12.5)
Servo system	TS1A02AA
Force sensor	Nitta IFS-67M25A25-I40

Fig. 7. Feedforward control block diagram.

2) A pair of antagonistic mono-articular motors (e_2–f_2) are connected by thrust wires to two pulleys fixed on joint 2. This motor pair produces the torque τ_2 about joint 2 as in Fig. 3.

3) A pair of antagonistic biarticular motors (e_3–f_3) are connected by mean of polyethylene wires to pulleys fixed on joint 2, and to free pulleys about joint axis 1. This motor pair produces the torque τ_3 about joint 1 and 2 as in Fig. 3.

Main characteristics of BiWi and of the actuator and sensor systems are shown in Tables II and III, respectively. Further details are available in [39].

The greater solution space of the ∞-norm model holds also for $\mathbb{R}^3$, which represents the mathematical space of the redundancy resolution problem in this study.

V. EXPERIMENTAL SETUP

A. BiWi: A Biarticularly Actuated and Wire Driven Robot Arm

BiWi robot arm, shown in Fig. 5, is used to experimentally validate the proposed ∞-norm approach, and compare it with the 2-norm approach. BiWi is a two-link planar manipulator actuated by six motors, each representing one of the six muscles in Fig. 1. The power is transmitted to the joints through pulleys and polyethylene wires as shown in Fig. 6.

1) A pair of antagonistic monoarticular motors (e_1–f_1) are connected by mean of polyethylene wires to two pulleys fixed on joint 1. This motor pair produces the torque τ_1 about joint 1 as in Fig. 3.
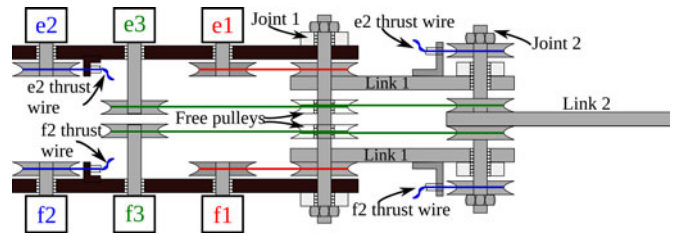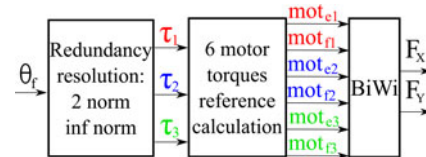
B. Feedforward Control Strategy

The feedforward control strategy used to collect the experimental data is shown in Fig. 7. Both the 2-norm and the ∞-norm approaches determine the joint actuator torques given a desired end effector force using a closed form solution. However, as the maximum end effector force is the object of study, the desired joint actuator torques τ_1, τ_2, and τ_3 that produce the maximum end effector force are calculated using an algorithm as in the following. Given a desired force angle θ_f and a redundancy resolution approach (2-norm or ∞-norm), the desired joint actuator torques (τ_1, τ_2, and τ_3) producing the maximum force in direction θ_f, while respecting the torque limits ($\tau_1^{\max}$, $\tau_2^{\max}$, and $\tau_3^{\max}$) are calculated using the following algorithm. For $\theta_f = k$:

TABLE IV
CALCULATION OF MOTOR INPUT REFERENCES FROM JOINT
ACTUATOR TORQUES

mot_{e1}	mot_{f1}	mot_{e2}	mot_{f2}	mot_{e3}	mot_{f3}
$(\tau_1)^-$	$(\tau_1)^+$	$K_{tl}(\tau_2)^-$	$K_{tl}(\tau_2)^+$	$(\tau_3)^-$	$(\tau_3)^+$

1) Set $i = 0$, and $|\mathbf{F}|_i = 0.001$
2) Calculate $\mathbf{T}_i$ using the Jacobian (7)
3) Given $\mathbf{T}_i$, calculate the necessary $(\tau_1)_i$, $(\tau_2)_i$ and $(\tau_3)_i$ using either the 2-norm approach [(9), (10), and (11)] or the ∞-norm approach [(22), (23), and (24)]
4) If $(|(\tau_1)_i| > \tau_1^{\max})$ or $(|(\tau_2)_i| > \tau_2^{\max})$ or $(|(\tau_3)_i| > \tau_3^{\max})$ then $(\tau_1)_i = (\tau_1)_{i-1}$, $(\tau_2)_i = (\tau_2)_{i-1}$, $(\tau_3)_i = (\tau_3)_{i-1}$ else $|\mathbf{F}| = |\mathbf{F}| + 0.001$, $i = i + 1$, and repeat from step 2
5) The calculated $(\tau_1)_i$, $(\tau_2)_i$, and $(\tau_3)_i$ are used as input reference torques.

The six motor reference torques are calculated using Table IV, where $(\tau_i)^+ = \max(0, \tau_i)$ and $(\tau_i)^- = \max(-\tau_i, 0)$ for $i = (1, 2, 3)$.

In order to compensate for the inevitable transmission loss in the thrust wires the reference motor torques for joint 2—mot_{e2} and mot_{f2}—are multiplied by a constant $K_{tl} = 1.33$. Such value is relatively high, due to the low cost of the thrust wires. However, by using more sophisticated thrust wires the transmission loss can be reduced to smaller value.

The desired reference motor torques [mot_{ei} and mot_{fi} for $i = (1, 2, 3)$] are sent to the robot arm as step inputs. The manipulator end effector output force ($\mathbf{F} = [F_x, F_y]^T$) is measured by a force sensor, and its steady state value is taken into account. The desired end effector output force direction θ_f varies from 0 to 360° every 5°.

VI. RESULTS

The joint actuator input torque patterns calculated using both the 2-norm and the ∞-norm approaches, as well as the calculated and measured maximum output force at the end effector of BiWi, obtained using these torque patterns are shown in Fig. 8(a) for $\theta_1 = -60°$ and $\theta_2 = 120°$, and in Fig. 8(b) for $\theta_1 = -25°$ and $\theta_2 = 50°$. In both cases, $\tau_1^{\max} = \tau_3^{\max} = 1.84$ Nm and $\tau_2^{\max} = 1.38$ Nm.

The experimental results agree with the calculated values, and show that the maximum output force at the end effector is greater when using the ∞-norm approach.

The relative difference in maximum output force magnitude expressed by

$$F^{\text{diff}} = \frac{|F_{\infty-n}^{\max}| - |F_{2-n}^{\max}|}{|F_{2-n}^{\max}|} \quad (32)$$

for the two approaches is shown in Fig. 8(a) and (b) for the two configurations. The ∞-norm approach allows a maximum end effector force greater (up to 35%) than the 2-norm approach.

VII. CONCLUSION

In this paper, a new approach based on ∞-norm to resolve actuator redundancy for robot arms driven by biarticular actuators

is proposed. A closed form solution based on a piecewise linear function for the proposed method is derived. The piecewise linear function is continuous in all its domain.

The proposed approach is compared with the traditional Moore–Penrose pseudoinverse approach (2-norm), by both calculation and experiment. Under the same maximum joint actuator torques, the proposed approach allows to obtain a greater output force at the end effector (up to 35%). Conversely, given a desired output force, by using the ∞-norm approach a smaller maximum joint actuator torque is required. Consequently, the ∞-norm approach allows the minimization of actuator size.

BiWi, a biarticularly actuated and wire driven manipulator, and a feedforward control strategy are used to experimentally validate the calculation.

In the future, the advantages of the proposed solution for three inputs and two outputs as, for example, parallel manipulators with a redundant DOF [12], or pen-based force display for precision manipulation in virtual environments [40], will be investigated in detail.

APPENDIX A

PROOF OF CLOSED FORM SOLUTION FOR THE 2-NORM APPROACH

The problem expressed by (8) is written for a simpler notation as follows:

$$\min \quad \sqrt{\frac{(x)^2}{(mx)^2} + \frac{(y)^2}{(my)^2} + \frac{(z)^2}{(mz)^2}}$$

$$\text{s.t.} \quad T_1 = x + z$$

$$T_2 = y + z \quad (33)$$

where T_1 and T_2 are the desired joint torques (known), x, y, and z are the desired joint actuator torques τ_1, τ_2, and τ_3 (unknown), respectively; $mx = \tau_1^{\max}$, $my = \tau_2^{\max}$, and $mz = \tau_3^{\max}$.

Taking into account $\mathbb{R}^3$, the solution (x, y, z) which satisfy $\sqrt{\frac{(x)^2}{(mx)^2} + \frac{(y)^2}{(my)^2} + \frac{(z)^2}{(mz)^2}}$ has to meet the following three requirements.

1) To be on the line defined by

$$T_1 = x + z \quad (34)$$

$$T_2 = y + z. \quad (35)$$

2) To be on the ellipsoid surface defined by

$$\frac{x^2}{(mx)^2} + \frac{y^2}{(my)^2} + \frac{z^2}{(mz)^2} = k \quad (36)$$

where k is a constant.

3) The plane passing through the line defined by (34) and (35) has to be tangent to the ellipsoid defined by (36). Hence,

$$\frac{1}{(mx)^2} \frac{\partial x^2}{\partial x} + \frac{1}{(my)^2} \frac{\partial y^2}{\partial y} + \frac{1}{(mz)^2} \frac{\partial z^2}{\partial z} = 0. \quad (37)$$
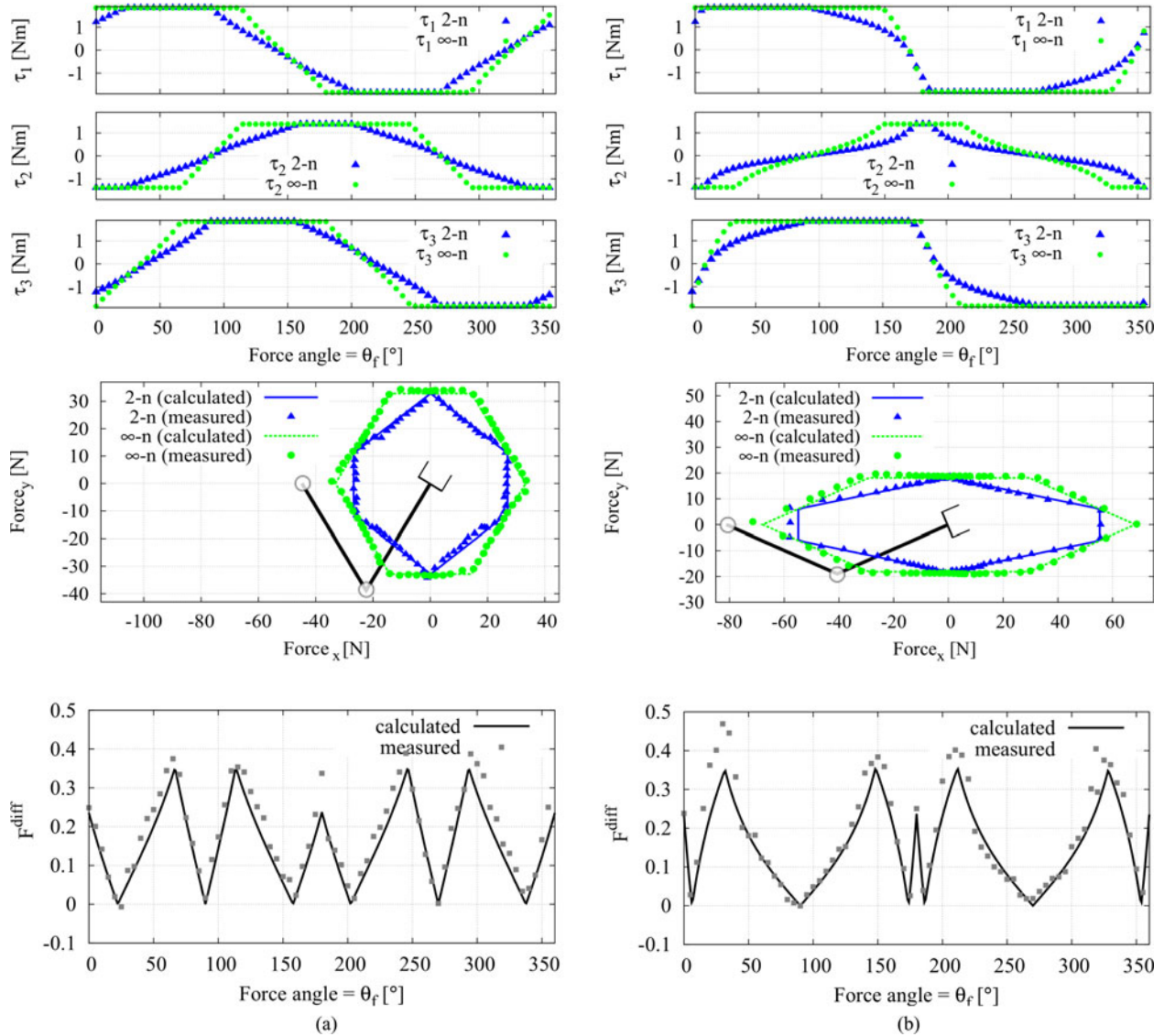
Fig. 8.   2-norm versus ∞-norm: joint actuator input torques (top), measured maximum output force (middle), relative difference in maximum output force (bottom). (a) $\theta_1 = -60°$ and $\theta_2 = 120°$. (b) $\theta_1 = -25°$ and $\theta_2 = 50°$.

Combining (34), (35), (36), and (37) straightforward follows the solution of the problem (33)

$$x = \frac{(T_1^- T_2)(mx)^2(mz)^2 + T_1^m x^2(my)^2}{(mx)^2(my)^2 + (mx)^2(mz)^2 + (my)^2(mz)^2} \quad (38)$$

$$y = \frac{T_2^m x^2(my)^2 + (T_2^- T_1)(my)^2(mz)^2}{(mx)^2(my)^2 + (mx)^2(mz)^2 + (my)^2(mz)^2} \quad (39)$$

$$z = \frac{T_1^m y^2(mz)^2 + T_2^m x^2(mz)^2}{(mx)^2(my)^2 + (mx)^2(mz)^2 + (my)^2(mz)^2}. \quad (40)$$

Equations (38), (39), and (40) correspond to (9), (10), and (11), respectively.

APPENDIX B
PROOF OF CLOSED-FORM SOLUTION
FOR THE ∞-NORM APPROACH

The problem expressed by (15) is written for a simpler notation as follows:

$$\min \quad \max \left(\frac{|x|}{mx}, \frac{|y|}{my}, \frac{|z|}{mz} \right)$$

$$\text{s.t.} \quad T_1 = x + z$$

$$T_2 = y + z \quad (41)$$

where T_1 and T_2 are the desired joint torques (known), x, y, and z are the desired joint actuator torques τ_1, τ_2, and τ_3 (unknown), respectively; $mx = \tau_1^{\max}$, $my = \tau_2^{\max}$, and $mz = \tau_3^{\max}$.

A closed form solution of (41) is determined in the following. The searched solution has to satisfy at least one of the three

equations $\frac{|x|}{mx} = \frac{|y|}{my}$, $\frac{|y|}{my} = \frac{|z|}{mz}$, $\frac{|x|}{mx} = \frac{|z|}{mz}$. In fact, when one of three variable's absolute value decreases at least one of the other two increases. Therefore, for any solution of the system with $\frac{|x|}{mx} \neq \frac{|y|}{my} \neq \frac{|z|}{mz}$ it is possible to decrease the higher value among the three so to be equal to at least one of the other two. Therefore, the searched solution is one among the following six:

1) $\frac{x}{mx} = -\frac{y}{my}$

$$\begin{cases} x + z = T_1 \\ y + z = T_2 \\ \frac{x}{mx} = -\frac{y}{my} \end{cases} \Rightarrow \begin{cases} x = (T_1 - T_2)\dfrac{mx}{my + mx} \\ y = (T_2 - T_1)\dfrac{my}{my + mx} \\ z = T_2 - (T_2 - T_1)\dfrac{my}{my + mx} \end{cases} \tag{42}$$

2) $\frac{y}{my} = \frac{z}{mz}$

$$\begin{cases} x + z = T_1 \\ y + z = T_2 \\ \frac{y}{my} = \frac{z}{mz} \end{cases} \Rightarrow \begin{cases} x = T_1 - T_2\dfrac{mz}{my + mz} \\ y = T_2\dfrac{my}{my + mz} \\ z = T_2\dfrac{mz}{my + mz} \end{cases} \tag{43}$$

3) $\frac{x}{mx} = \frac{z}{mz}$

$$\begin{cases} x + z = T_1 \\ y + z = T_2 \\ \frac{x}{mx} = \frac{z}{mz} \end{cases} \Rightarrow \begin{cases} x = T_1\dfrac{mx}{mz + mx} \\ y = T_2 - T_1\dfrac{mz}{mz + mx} \\ z = T_1\dfrac{mz}{mz + mx} \end{cases} \tag{44}$$

4) $\frac{x}{mx} = \frac{y}{my}$

$$\begin{cases} x + z = T_1 \\ y + z = T_2 \\ \frac{x}{mx} = \frac{y}{my} \end{cases} \Rightarrow \begin{cases} x = (T_2 - T_1)\dfrac{mx}{my - mx} \\ y = (T_2 - T_1)\dfrac{my}{my - mx} \\ z = T_2 - (T_2 - T_1)\dfrac{my}{my - mx} \end{cases} \tag{45}$$

5) $\frac{y}{my} = -\frac{z}{mz}$

$$\begin{cases} x + z = T_1 \\ y + z = T_2 \\ \frac{y}{my} = -\frac{z}{mz} \end{cases} \Rightarrow \begin{cases} x = T_1 - T_2\dfrac{mz}{mz - my} \\ y = -T_2\dfrac{my}{mz - my} \\ z = T_2\dfrac{mz}{mz - my} \end{cases} \tag{46}$$

6) $\frac{x}{mx} = -\frac{z}{mz}$

$$\begin{cases} x + z = T_1 \\ y + z = T_2 \\ \frac{x}{mx} = -\frac{z}{mz} \end{cases} \Rightarrow \begin{cases} x = -T_1\dfrac{mx}{mz - mx} \\ y = T_2 - T_1\dfrac{mz}{mz - mx} \\ z = T_1\dfrac{mz}{mz - mx}. \end{cases} \tag{47}$$

Among the six possible solutions the searched one is directly selected on the basis of T_1 and T_2 as follows (the variable subscript represents the respective equation number):

1) If $(T_1 \leq c_1 T_1$ and $T_2 \geq c_3 T_1)$ or $(T_1 > c_1 T_2$ and $T_2 < c_3 T_1)$,

$$\left|\frac{x_{(42)}}{mx}\right| = \left|\frac{y_{(42)}}{my}\right| \geq \left|\frac{z_{(42)}}{mz}\right| \tag{48}$$

$$|x_{(42)}| \leq |x_{(43)}| \tag{49}$$

$$|y_{(42)}| \leq |y_{(44)}| \tag{50}$$

$$|x_{(42)}| \leq |x_{(45)}| \tag{51}$$

$$|x_{(42)}| \leq |x_{(46)}|, \quad \text{if } mz \geq my \tag{52}$$

$$|y_{(42)}| \leq |y_{(46)}|, \quad \text{if } mz < my \tag{53}$$

$$|x_{(42)}| \leq |x_{(47)}|, \quad \text{if } mx \geq mz \tag{54}$$

$$|y_{(42)}| \leq |y_{(47)}|, \quad \text{if } mx < mz. \tag{55}$$

Therefore, solution is (42). In this case, τ_1 in (22), τ_2 in (23), and τ_3 in (24), are equal to x in (42), y in (42), and z in (42), respectively.

2) If $(T_1 \geq c_1 T_2$ and $T_2 \geq c_2 T_1)$ or $(T_1 < c_1 T_2$ and $T_2 < c_2 T_1)$,

$$\left|\frac{y_{(43)}}{my}\right| = \left|\frac{z_{(43)}}{mz}\right| \geq \left|\frac{x_{(43)}}{mx}\right| \tag{56}$$

$$|z_{(43)}| \leq |z_{(42)}| \tag{57}$$

$$|y_{(43)}| \leq |y_{(44)}| \tag{58}$$

$$|y_{(43)}| \leq |y_{(45)}|, \quad \text{if } my \geq mx \tag{59}$$

$$|z_{(43)}| \leq |z_{(45)}|, \quad \text{if } my < mx \tag{60}$$

$$|y_{(43)}| \leq |y_{(46)}| \tag{61}$$

$$|y_{(43)}| \leq |y_{(47)}|, \quad \text{if } mx \geq mz \tag{62}$$

$$|z_{(43)}| \leq |z_{(47)}|, \quad \text{if } mx < mz. \tag{63}$$

Therefore, solution is (43). In this case, τ_1 in (22), τ_2 in (23), and τ_3 in (24), are equal to x in (43), y in (43), and z in (43), respectively.

3) If $(T_2 \leq c_2 T_1$ and $T_2 \geq c_3 T_1)$ or $(T_2 > c_2 T_1$ and $T_2 < c_3 T_1)$,

$$\left|\frac{x_{(44)}}{mx}\right| = \left|\frac{z_{(44)}}{mz}\right| \geq \left|\frac{y_{(44)}}{my}\right| \tag{64}$$

$$|z_{(44)}| \leq |z_{(42)}| \tag{65}$$

$$|x_{(44)}| \leq |x_{(43)}| \tag{66}$$

$$|x_{(44)}| \leq |x_{(45)}|, \quad \text{if } mx \geq my \tag{67}$$

$$|z_{(44)}| \leq |z_{(45)}|, \quad \text{if } mx < my \tag{68}$$

$$|x_{(44)}| \leq |x_{(46)}|, \quad \text{if } my \geq mz \tag{69}$$

$$|z_{(44)}| \leq |z_{(46)}|, \quad \text{if } my < mz \tag{70}$$

$$|x_{(44)}| \leq |x_{(47)}|. \tag{71}$$

Therefore, solution is (44). In this case, τ_1 in (22), τ_2 in (23), and τ_3 in (24), are equal to x in (44), y in (44), and z in (44), respectively.

REFERENCES

[1] N. Hogan, "Impedance control: An approach to manipulation: Part I—Theory," *J. Dyn. Syst., Meas., Control*, vol. 107, no. 1, pp. 1–7, Mar. 1985.

[2] R. Patel, H. Talebi, J. Jayender, and F. Shadpey, "A robust position and force control strategy for 7-DOF redundant manipulators," *IEEE/ASME Trans. Mechatronics*, vol. 14, no. 5, pp. 575–589, Oct. 2009.

[3] G. White, R. Bhatt, C. Tang, and V. Krovi, "Experimental evaluation of dynamic redundancy resolution in a nonholonomic wheeled mobile manipulator," *IEEE/ASME Trans. Mechatronics*, vol. 14, no. 3, pp. 349–357, Jun. 2009.

[4] D. J. Braun, J. E. Mitchell, and M. Goldfarb, "Actuated dynamic walking in a seven-link biped robot," *IEEE/ASME Trans. Mechatronics*, vol. 17, no. 1, pp. 147–156, Feb. 2012.

[5] K. Yoshida, N. Hata, S. Oh, and Y. Hori, "Extended manipulability measure and application for robot arm equipped with bi-articular driving mechanism," in *Proc. 35th Annu. Conf. IEEE Ind. Electron. Soc.*, 2009, pp. 3083–3088.

[6] A. Z. Shukor and Y. Fujimoto, "Modelling and control of redundant robot manipulator using spiral motor," in *Proc. 6th Eur.-Asia Congr. Mechatron.*, 2010, pp. 59–65.

[7] L. Wang, J. Wu, J. Wang, and Z. You, "An experimental study of a redundantly actuated parallel manipulator for a 5-DOF hybrid machine tool," *IEEE/ASME Trans. Mechatronics*, vol. 14, no. 1, pp. 72–81, Feb. 2009.

[8] C. A. Klein and C. H. Huang, "Review of pseudoinverse control for use with kinematically redundant manipulators," *IEEE Trans. Syst., Man, Cybern.*, vol. 13, pp. 245–250, 1983.

[9] I. Shim and Y. Yoon, "Stabilized minimum infinity-norm torque solution for redundant manipulators," *Robotica*, vol. 16, no. 02, pp. 193–205, 1998.

[10] A. S. Deo and I. D. Walker, "Minimum effort inverse kinematics for redundant manipulators," *IEEE Trans. Robot. Autom.*, vol. 13, no. 5, pp. 767–775, Oct. 1997.

[11] H. Ding and J. Wang, "Recurrent neural networks for minimum infinity-norm kinematic control of redundant manipulators," *IEEE Trans. Syst., Man Cybern.*, vol. 29, no. 3, pp. 269–276, May 1999.

[12] X. Zhu, G. Tao, B. Yao, and J. Cao, "Adaptive robust posture control of parallel manipulator driven by pneumatic muscles with redundancy," *IEEE/ASME Trans. Mechatronics*, vol. 13, no. 4, pp. 441–450, Aug. 2008.

[13] H. Fukusho, T. Sugimoto, and T. Koseki, "Control of a straight line motion for a two-link robot arm using coordinate transform of bi-articular simultaneous drive," in *Proc. 11th IEEE Int. Workshop Adv. Motion Control*, 2010, pp. 786–791.

[14] M. Kumamoto, T. Oshima, and T. Yamamoto, "Control properties induced by the existence of antagonistic pairs of bi-articular muscles—Mechanical engineering model analyses," *Human Movement Sci.*, vol. 13, no. 5, pp. 611–634, Oct. 1994.

[15] S. Oh, V. Salvucci, Y. Kimura, and Y. Hori, "Development of simplified statics of robot manipulator and optimized muscle torque distribution based on the statics," in *Proc. Amer. Control Conf*, 2011, pp. 4099–4104.

[16] V. Salvucci, Y. Kimura, S. Oh, and Y. Hori, "Experimental verification of infinity norm approach for precise force control of manipulators driven by bi-articular actuators," in *Proc. Int. Federat. Automat. Control*, 2011, pp. 13510–13515.

[17] T. Tsuji, "A model of antagonistic triarticular muscle mechanism for lancelet robot," in *Proc. 11th IEEE Int. Workshop Adv. Motion Control*, 2010, pp. 496–501.

[18] V. Salvucci, Y. Kimura, S. Oh, and Y. Hori, "Disturbance rejection improvement in Non-Redundant robot arms using bi-articular actuators," in *Proc. IEEE Int. Symp. Ind. Electron.*, 2011, pp. 2159–2164.

[19] K. Yoshida, T. Uchida, and Y. Hori, "Novel FF control algorithm of robot arm based on bi-articular muscle principle-emulation of muscular viscoelasticity for disturbance suppression and path tracking," in *Proc. 33th Annu. Conf. IEEE Ind. Electron. Soc.*, 2007, pp. 310–315.

[20] S. Oh, Y. Kimura, and Y. Hori, "Reaction force control of robot manipulator based on biarticular muscle viscoelasticity control," in *Proc. IEEE/ASME Int. Conf. Adv. Intell. Mech.*, 2010, pp. 1105–1110.

[21] G. J. Van Ingen Schenau, "From rotation to translation: Constraints on multi-joint movements and the unique action of bi-articular muscles," *Human Movement Sci.*, vol. 8, no. 4, pp. 301–337, Aug. 1989.

[22] J. Babic, B. Lim, D. Omrcen, J. Lenarcic, and F. Park, "A biarticulated robotic leg for jumping movements: Theory and experiments," *J. Mech. Robot.*, vol. 1, no. 1, pp. 011013-1–011013-9, 2009.

[23] K. Hosoda, Y. Sakaguchi, H. Takayama, and T. Takuma, "Pneumatic-driven jumping robot with anthropomorphic muscular skeleton structure," *Auton. Robots*, vol. 28, no. 3, pp. 307–316, Dec. 2009.

[24] M. A. Lewis, M. R. Bunting, B. Salemi, and H. Hoffmann, "Toward ultra high speed locomotors: Design and test of a cheetah robot hind limb," in *Proc. IEEE Int. Conf. Rob. Autom.*, 2011, pp. 1990–1996.

[25] T. Oshima, N. Momose, K. Koyanagi, T. Matsuno, and T. Fujikawa, "Jumping mechanism imitating vertebrate by the mechanical function of bi-articular muscle," in *Proc. Int. Conf. Mechatron. Autom.*, 2007, pp. 1920–1925.

[26] R. Niiyama, S. Nishikawa, and Y. Kuniyoshi, "Athlete robot with applied human muscle activation patterns for bipedal running," in *Proc. 10th IEEE-RAS Int. Conf. Humanoid Robots*, 2010, pp. 498–503.

[27] Y. Shibata, S. Imai, T. Nobutomo, T. Miyoshi, and S. Yamamoto, "Development of body weight support gait training system using antagonistic bi-articular muscle model," in *Proc. IEEE Annu. Int. Conf. Eng. Med. Biol. Soc.*, 2010, pp. 4468–4471.

[28] K. Tadano, M. Akai, K. Kadota, and K. Kawashima, "Development of grip amplified glove using bi-articular mechanism with pneumatic artificial rubber muscle," in *Proc. IEEE Int. Conf. Rob. Autom.*, 2010, pp. 2363–2368.

[29] T. Fujikawa, T. Oshima, M. Kumamoto, and N. Yokoi, "Output force at the endpoint in human upper extremities and coordinating activities of each antagonistic pairs of muscles," *Trans. Jpn. Soc. Mech. Eng.*, vol. 65, no. 632, pp. 1557–1564, 1999.

[30] P. Culmer, A. Jackson, S. Makower, R. Richardson, J. Cozens, M. Levesley, and B. Bhakta, "A control strategy for upper limb robotic rehabilitation with a dual robot system," *IEEE/ASME Trans. Mechatronics*, vol. 15, no. 4, pp. 575–585, Aug. 2010.

[31] T. Noritsugu and T. Tanaka, "Application of rubber artificial muscle manipulator as a rehabilitation robot," *IEEE/ASME Trans. Mechatronics*, vol. 2, no. 4, pp. 259–267, Dec. 1997.

[32] A. Chiri, N. Vitiello, F. Giovacchini, S. Roccella, F. Vecchi, and M. C. Carrozza, "Mechatronic design and characterization of the index finger module of a hand exoskeleton for post-stroke rehabilitation," *IEEE/ASME Trans. Mechatronics*.

[33] K. Kong, J. Bae, and M. Tomizuka, "A compact rotary series elastic actuator for human assistive systems," *IEEE/ASME Trans. Mechatronics*, vol. 17, no. 2, pp. 1–10, Apr. 2010.

[34] S. Banala, S. Agrawal, S. H. Kim, and J. Scholz, "Novel gait adaptation and neuromotor training results using an active leg exoskeleton," *IEEE/ASME Trans. Mechatronics*, vol. 15, no. 2, pp. 216–225, 2010.

[35] S. Shimizu, N. Momose, T. Oshima, and K. Koyanagi, "Development of robot leg which provided with the bi-articular actuator for training techniques of rehabilitation," in *Proc. IEEE Int. Workshop Robot Human Interact. Commun.*, 2009, pp. 921–926.

[36] A. Umemura, Y. Saito, and K. Fujisaki, "A study on power-assisted rehabilitation robot arms operated by patient with upper limb disabilities," in *Proc. IEEE Int. Conf. Rehabil. Robot.*, 2009, pp. 451–456.

[37] V. Salvucci, Y. Kimura, S. Oh, and Y. Hori, "Experimental verification of infinity norm approach for force maximization of manipulators driven by bi-articular actuators," in *Proc. Amer. Control Conf.*, 2011, pp. 4105–4110.

[38] V. Salvucci, S. Oh, and Y. Hori, "Infinity norm approach for precise force control of manipulators driven by bi-articular actuators," in *Proc. IEEE 36th Annu. Conf. Ind. Electron*, 2010, pp. 1908–1913.

[39] V. Salvucci, Y. Kimura, S. Oh, and Y. Hori, "BiWi: Bi-Articularly actuated and wire driven robot arm," in *Proc. IEEE Int. Conf. Mechatronics*, 2011, pp. 827–832.

[40] P. Buttolo and B. Hannaford, "Pen-based force display for precision manipulation in virtual environments," in *Proc. IEEE Virtual Reality Annu. Int. Symp.*, 1995, pp. 217–224.

Valerio Salvucci (S'10–M'12) received the B.S. and M.S. degrees in industrial engineering from the University of Pisa, Pisa, Italy, in 2004, and from the University of Bologna, Bologna, Italy, in 2008, respectively, and the Ph.D. degree in electrical engineering from The University of Tokyo, Tokyo, Japan.

He is currently a Fellow Researcher in the Department of Advanced Energy, The University of Tokyo. His research interests include motion control, biologically inspired robotics, redundant systems, and human-friendly power-assist robotics.

Yasuto Kimura received the B.S. degree in electrical engineering and the M.S. degree in frontier sciences from The University of Tokyo, Tokyo, Japan, in 2010 and 2012, respectively.

He is currently with the Department of Advanced Energy, The University of Tokyo. His research fields include motion control and biologically inspired robotics.

Yoichi Hori (S'81–M'83–SM'00–F'05) received the B.S., M.S., and Ph.D. degrees in electrical engineering from The University of Tokyo, Tokyo, Japan, in 1978, 1980, and 1983, respectively.

In 1983, he joined the Department of Electrical Engineering, The University of Tokyo, as a Research Associate. He later became an Assistant Professor, an Associate Professor, and, in 2000, a Professor at the same university. In 2002, he was with the Institute of Industrial Science as a Professor in the Information and System Division, and in 2008, with the Department of Advanced Energy, Graduate School of Frontier Sciences, The University of Tokyo, where he is currently with the Department of Electrical Engineering. From 1991 to 1992, he was a Visiting Researcher at the University of California at Berkeley. His research interests include control theory and its industrial applications to motion control, mechatronics, robotics, electric vehicles, etc.

Dr. Hori has been the Treasurer of the IEEE Japan Council and Tokyo Section since 2001. He was the winner of the Best Transactions Paper Award from the IEEE TRANSACTIONS ON INDUSTRIAL ELECTRONICS in 1993 and 2001, of the 2000 Best Transactions Paper Award from the Institute of Electrical Engineers of Japan (IEEJ), and 2011 Achievement Award of the IEEJ. He is an AdCom member of the IEEE Industrial Electronics Society. He is also a member of the Society of Instrument and Control Engineers; The Robotics Society of Japan; Japan Society of Mechanical Engineers; and the Society of Automotive Engineers of Japan. He is the ex-President of the Industry Applications Society of the IEEJ, the President of the Capacitors Forum, and the Chairman of the Motor Technology Symposium of the Japan Management Association and the Director of Technological Development of the SAE-Japan.

Sehoon Oh (S'05–M'06) received the B.S., M.S., and Ph.D. degrees in electrical engineering from The University of Tokyo, Tokyo, Japan, in 1998, 2000, and 2005, respectively.

After his career as a Research Professor in the Department of Electrical Engineering, The University of Tokyo, he is now a Senior Engineer in Samsung Heavy Industries. His research fields include the development of human-friendly motion control algorithms and assistive devices for people.

Dr. Oh is a member of the Institute of Electrical Engineers of Japan, the Society of Instrument and Control Engineers, and The Robotics Society of Japan.